Electron density measurements in detached divertor plasmas of ASDEX Upgrade via Stark broadening of the Balmer lines

S. Potzel, R. Dux, H.W. Müller, A. Scarabosio, M. Wischmeier and ASDEX Upgrade team

Max-Planck-Institut für Plasmaphysik, EURATOM Association, Garching, Germany

Introduction

In ITER, in order to be able to handle the particle and power fluxes to the target material, the divertor has to be operated with the plasma detached or semi-detached from the target. Thus, understanding the physics of detachment is crucial to make predictions for the ITER divertor. In the detached regime, the region of high electron density (n_e) is retracted from the target and the commonly used Langmuir probes do not provide information about the plasma in the divertor volume. In this context, a new spectroscopic method has been developed to determine n_e in the divertor of ASDEX Upgrade, using the Stark broadening of the Balmer lines.

After introducing this method, measurements of a detached divertor plasma are presented. Finally, it is shown how impurity seeding can change the detached divertor plasma.

Electron density determination using Stark broadening of the Balmer lines

The statistically distributed electrons and ions in the divertor disturb the emitting D atoms in two ways. The fast particles collide with the atom, which leads to pressure broadening and thus to a Lorentz profile, depending on n_e (assuming $n_e = n_{ion}$). The more static particles produce electric micro fields of various strength leading to the Stark splitting. Here, the profile is the result of the splitting for all E-field strengths multiplied by its probability to occur. This probability distribution also depends on n_e. The total broadening is a combination of both, the Lorentz profile, valid in the line centre and the static Stark profile, determining the line wings. Griem has given a quantum mechanical approach (see [1] and references therein) to calculate these profiles, but the pressure broadening due to fast ions was neglected. A different approach is the so called Model Microfield Method (MMM). Here, the E-field strength jumps in a statistical manner and independent for electrons and ions [2]. Thus, the fast ions are taken into account. For higher upper principal quantum numbers of the radiative transition, the Stark broadening becomes larger. Therefore D_ε ($n = 7 \rightarrow n = 2$) has been used for the n_e evaluation. D_ε profiles have been calculated following Griem's approach and compared to profiles published by Stehlé [3] based on the MMM. For this line, both theories agree very well for typical n_e values in the divertor plasma (see Fig. 1a).

Due to the B-fields (≈ 2.5T) in the Tokamak, the influence of an additional Zeeman splitting on the profile has to be checked. This can be done in Griem's approach by adding an additional perturbation operator [4]. Based on this, line shapes have been calculated without and with additional Zeeman splitting (Fig. 1b). Here it is shown, that for typical parameters the Zeeman splitting can be neglected compared to the Stark broadening of D_ε. Because MMM profiles are today the most accurate claiming an uncertainty of $\approx 10\%$, these profiles, neglecting the Zeeman splitting, have been used for the n_e determination.

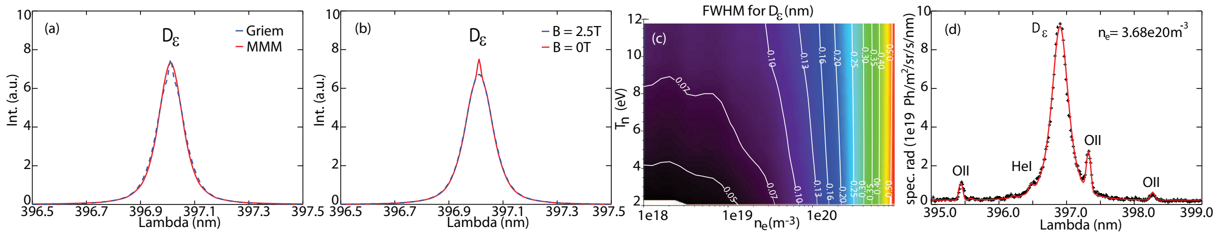

Figure 1: (a) D_ε profile for $n_e = 1 \cdot 10^{20}\mathrm{m}^{-3}$ calculated with Griem's approach (blue) and with MMM (red), (b) D_ε profile calculated with Griem's approach for $n_e = 1 \cdot 10^{20}\mathrm{m}^{-3}$, $B = 0$T (red) and $B = 2.5$T (blue), (c) $FWHM$ of D_ε over n_e and T_n, (d) fit on D_ε of a measured spectrum

The Doppler broadening due to the temperature T_n of the D atom must also be taken into account by folding the Gaussian Doppler profile with the Stark profile. In Fig. 1c the full width at half maximum ($FWHM$) of a Stark and Doppler broadened D_ε line is calculated for typical ranges of n_e and T_n. For $n_e \geq 3 \cdot 10^{19}\mathrm{m}^{-3}$ the $FWHM$ is insensitive to small changes of T_n around $\approx 5eV$, which sets the lower boundary of this method.

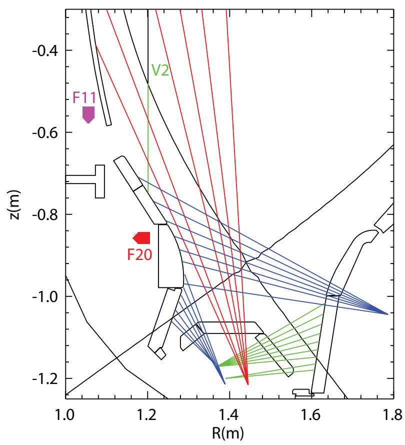

Figure 2: Geometry of LOS. Also shown are pressure gauges (F11 & F20) and an interferometer cord (V2)

The theoretical D_ε profile is finally a convolution of the Stark profile, the Doppler profile with $T_n = 5$eV (close to Franck-Condon dissociation energy of recycled D_2) and the well known spectrometer function. The total spectrum contains furthermore oxygen lines from a multiplet of OII with fixed line ratio and a HeI line. This theoretical spectrum is fitted in a least square sense to the measured data where n_e and the line intensities are fit parameters (Fig. 1d).

These spectra are simultaneously measured on up to 25 lines of sight (LOS) with a time resolution of 2.65ms. The geometry of the LOS is shown in Fig. 2. This allows especially for the inner divertor the determination of n_e in the divertor volume with a very good spatial coverage. The influence of stray radiation due to the high reflectivity of the tungsten tiles and the strong n_e and T_e gradients in the divertor plasma has to be minimized. Thus, the LOS are installed such that they end in a viewing dump between two divertor tiles. It should be noted that this is not a line integrated measurement of n_e but a measurement weighted with the D_ε emissivity in the integral along the LOS.

Divertor detachment

A gas fuelling ramp was applied during L-mode discharge at $I_p = 1$MA, $B_T = 2.5$T and with additional ECRH power of 600kW. The fuelling ramp leads to a continuous increase of the line integrated plasma density (Fig. 3a) and drives both divertors from the high recycling regime to complete detachment.

In Fig. 3b-i measurements of n_e and radiance of D_ε measured with Stark broadening and ion saturation current (j_{sat}) measured by Langmuir probes are shown for both divertors. The ΔS co-ordinate is the poloidal distance from the strike-point along the divertor surface, positive values are in the SOL. ΔR is the distance from the x-point along a horizontal line, negative values are in the inner SOL.

With increasing plasma density, j_{sat} is increasing, too, until it saturates and finally decreases (Fig. 3b,e). This 'roll-over', starting first in the inner divertor, denotes the onset of detachment. This phase is connected with a strong increase of n_e in the inner and outer divertor volume (Fig. 3c,f). Also a second peak appears in the inner divertor far SOL (Fig. 3e,f) and near the x-point (Fig. 3h). As detachment proceeds, j_{sat} at the strike zone finally vanishes, a condition often named complete detachment. During this phase n_e in the divertor volume further increases and moves upwards. With the horizontal and vertical LOS in the inner divertor, it can be shown that this front moves towards the x-point and not along the target (Fig. 3f,h). When the high n_e front has moved away from the target D_ε increases strongly (Fig. 3d,g,i). This indicates a high neutral density and recombination in this region (D_ε radiation is strongly induced by recombination), as previously observed in [5].

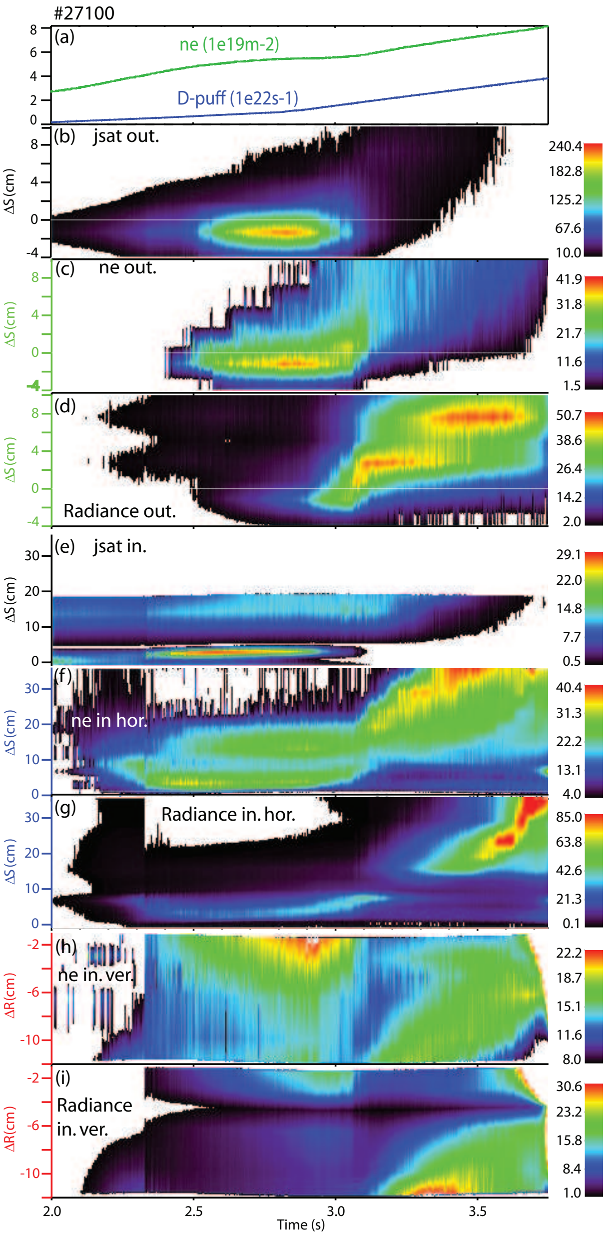

Figure 3: Time traces of (a) plasma fuelling (blue) and main averaged density (green); (b,e) j_{sat} in $1\cdot10^{21}\mathrm{m}^{-2}\mathrm{s}^{-1}$ for the inner and outer target; (c,f,h) n_e in $1\cdot10^{19}\mathrm{m}^{-3}$ and (d,g,i) D_ε radiance in $1\cdot10^{21}\mathrm{Ph/m^2/s/sr}$ for the outer, inner horizontal and vertical LOS, respectively (The colour of the spatial co-ordinate refers to the LOS in Fig. 2)

Effect of N_2 seeding on the inner divertor plasma

Nitrogen seeding is routinely used in ASDEX Upgrade high power H-mode discharges to cool the divertor plasma via radiation and to reduce the power load to the outer divertor target [6]. N_2 seeding also changes the inner detached divertor plasma. In phases without N_2 seeding a large n_e around $5\cdot10^{20}\mathrm{m}^{-3}$ is measured in the far SOL via Stark broadening and a vertical interferometer cord (Fig. 4b,c,d). Knowing the density profile of the confined plasma, one can subtract this part from the interferometer measurement, giving the line averaged density in the far SOL [7]. With an intersection length of $\approx 10cm$ of the cord in the SOL (green line in Fig. 2), n_e of the order of $1 \cdot 10^{20}\mathrm{m}^{-3}$ are measured, in line with the Stark measurements. Moreover, high neutral fluxes (Γ_D) are measured with fast ion gauges in the near and far SOL (Fig. 4b). Applying a constant N_2 puff into the divertor leads to a strong reduction of both, n_e ($\approx 70\%$) and Γ_D ($\approx 50\%$) in the far SOL. Also the region of high n_e and Γ_D does not extend to the far SOL anymore but concentrates closer to the x-point. This is consistent with the reconstructed radiation from bolometry. When the heating power is increased by 2.5MW, the previous distribution is reestablished.

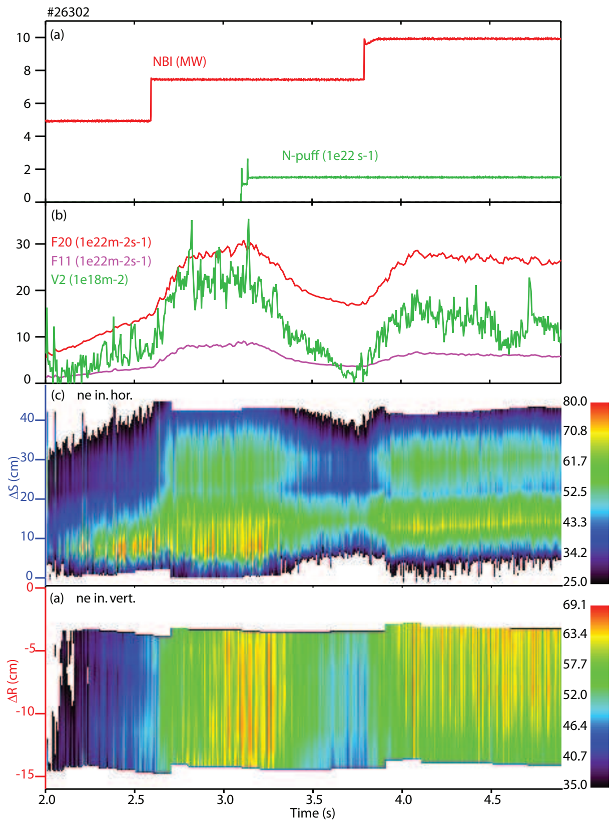

Figure 4: Time traces of (a) NBI heating (red), N_2 puff (green); (b) Γ_D (red & magenta), n_e from V2; n_e from Stark broadening for the inner horizontal (c) and vertical (d) LOS in $1 \cdot 10^{19}\mathrm{m}^{-3}$ (The colour of the spatial co-ordinate refers to the LOS in Fig. 2)

Conclusion

A new spectroscopic method determining n_e in the divertor has been developed for ASDEX Upgrade. This provides information about n_e in the divertor volume, being of special interest in detached plasmas when the Langmuir probes can no longer measure n_e. With this diagnostic the movement of the n_e front to the x-point and the formation of a zone with high neutral density situated between the front and the target has been measured during the plasma development towards complete detachment.

Large n_e and Γ_D in the far SOL are measured in high power H-mode discharges, consistent with interferometric and neutral flux measurements. N_2 seeding reduces the extension into the far SOL, and the high n_e region moves towards the x-point.

References

[1] H.R. Griem, Plasma Spectroscopy, McGraw-Hill Book Company, (1997)
[2] U. Frisch and A. Brissaud, J. Quant. Spectrosc. Radiat. Transfer, **1753:1766**, 11 (1971)
[3] C. Stehlé and R. Hutcheon, Astron. Astrophys. SuppL. Ser., **93:97**, 140 (1999)
[4] Nguyen-Hoe, et al., J. Quant. Spectrosc. Radiat. Transfer, **429:474**, 7 (1967)
[5] A. Scarabosio, J. Nucl. Mater., **390-391**, 494 (2009).
[6] A. Kallenbach, Plasma Phys. Control. Fusion, **52**, 055002 (2010)
[7] K. McCormick, J. Nucl. Mater., **390-391**, 465 (2009).